Electric-field-induced Γ-X mixing between Stark ladders in short-period GaAs/AlAs superlattices

M. Morifuji, M. Yamaguchi, K. Taniguchi, and C. Hamaguchi
Department of Electronic Engineering, Faculty of Engineering, Osaka University, Yamada-oka, Suita, Osaka 565, Japan
(Received 7 March 1994)

Electronic structures of short-period GaAs/AlAs superlattices in a uniform electric field along the growth axis are studied by a second-neighbor tight-binding method. Minibands of the X band edge in AlAs show discrete energy levels, the so-called Stark ladder, as do the Γ minibands in GaAs. Electric-field-induced mixing between a Stark ladder of the Γ miniband and one of the X miniband is studied and found to depend strongly on miniband indices and superlattice structures. The optical transition probability between the Stark ladder of valence states and that of the X miniband is strongly enhanced due to the Γ-X mixing.

I. INTRODUCTION

The energy spectrum of a solid under a strong electric field F is quite different from that of Bloch states. Under an electric field the energies are given by $E(n) = nedF$, where n is an integer, e is the electron charge and d is the lattice constant. These discrete energy levels are associated with localized states with the localization length $\lambda = W/(2eF)$ where W is the bandwidth. These localized states, which are called Stark ladders, are induced when the electrostatic energy is larger than the bandwidth,

$$W < eFd. \tag{1}$$

Since Wannier pointed out the existence of a Stark ladder in a crystalline solid, it has attracted much attention.[1] Zak argued that the localized states cannot exist in a solid because the interband coupling destroys the localized character of the states.[2] Some authors have carried out theoretical studies based on the one-dimensional tight-binding model with interband coupling, and confirmed the existence of Stark ladders.[3–5] Thus, the Stark ladder is widely believed to exist even if the interband coupling is strong when the condition of Eq. (1) is satisfied. On the other hand, there have been few experimental works to observe the Stark ladders because the electric field needed to induce the Stark ladders is too large in a bulk material. Only an oscillatory behavior of conductivity in ZnS was considered a sign of the Stark ladders.[6]

Recently, however, the Stark ladders were observed in GaAs/AlAs superlattices.[7–15] This is due to the fact that a small bandwidth associated with a large lattice constant of a superlattice reduces the strength of the electric field to induce Stark ladders, hence the Stark ladders easily occur. The Stark ladders in GaAs/AlAs superlattices have attracted much attention and have been intensively studied both theoretically and experimentally. In order to understand the behavior of the Stark ladders, a realistic band structure is necessary. Energy spectra of Stark ladders have been studied theoretically with methods such as the effective-mass approximation[14,16] and the tight-binding method.[3,5,17,18] Although the effective-mass approximation is convenient for calculating the energy spectra, it is difficult to include some important effects such as interband mixing between Stark ladders of different valleys. On the other hand, the tight-binding method has the capability to produce realistic band structures with the appropriate choice of empirical parameters.[19–22] We have already reported that Stark ladders can be well described by a tight-binding picture with the effects of the electric field included as diagonal elements of a Hamiltonian matrix.[17] From the tight-binding calculation, we have also found that the spin-orbit split-off band in the valence band forms the Stark ladder, although it has energies larger than the potential barrier.[23]

The energy bands of superlattices are quite complicated due to many minibands folded into the first Brillouin zone. For a short-period $(GaAs)_n/(AlAs)_n$ superlattice with n=5–15, in particular, the X miniband of AlAs is close in terms of energy to the Γ miniband of GaAs. Much effort has been made to study the alignment of the X_{xy} band edge, the X_z band edge, and the Γ band edge, and it is widely accepted that the lowest conduction miniband is X_z for n smaller than 12 and is Γ state for n larger than 13. Electric-field-induced mixing between the Stark ladders of the Γ band edge and those of the X band edge is of interest. In this paper we focus our attention on Stark ladders of short-period $(GaAs)_n/(AlAs)_n$ superlattices (n=8–12) in which the X_z miniband of AlAs is close in terms of energy to the Γ miniband of GaAs. We investigate the effect of the electric-field-induced Γ-X mixing on Stark ladders by using the tight-binding method.

II. TIGHT-BINDING MODEL

We consider a $(GaAs)_n/(AlAs)_n$ superlattice in an electric field along the growth axis (z axis). The Hamiltonian we consider is given by

$$\mathcal{H} = \sum_{i,j,m,n} t_{im;jn} a^{\dagger}_{im} a_{jn} + \sum_{i,m} \epsilon_{im} a^{\dagger}_{im} a_{im} + eF \sum_{i,m} z_i a^{\dagger}_{im} a_{im}. \quad (2)$$

In Eq. (2), $a^{\dagger}_{im}(a_{im})$ is a creation (annihilation) operator of the mth orbital at the ith atomic site, $\phi_m(\boldsymbol{r} - \boldsymbol{r}_i)$ (m stands for s, p_x, p_y, and p_z) with an assumption of orthogonality between them.[24] $t_{im;jn}$ and ϵ_{im} are the transfer integrals and the site energies, respectively. In order to obtain a good description of the Stark ladder of the X band edge, it is necessary to reproduce correct band structure at the X point. The first-neighbor tight-binding model leads to an artificial dispersionless band along the X-W line, and thus the band structure near the X point is incorrect. Some authors tried to produce good band at the X point by extending the interaction up to the second-neighboring atoms.[20–22] Among them, Lu and Sham presented a new set of tight-binding parameters so as to reproduce the effective masses at some points in the first Brillouin zone as well as the energies, and they explained that the alignment between the X_z band edge and the Γ band edge changes at n=12 for $(GaAs)_n/(AlAs)_n$ superlattices. This interpretation was confirmed by comparison of the calculation with the experimental data by Matsuoka *et al.*[25] Since Stark ladders are affected by the effective mass at the band edge, we use the tight-binding parameters obtained for GaAs and AlAs by Lu and Sham so as to obtain Stark ladders of X minibands of AlAs. We simply averaged tight-binding parameters at the interfaces between GaAs and AlAs because the superlattice period we consider is not very short. The third term of Eq. (2) denotes the potential energy of atomic orbitals due to the electric field.

In the normal tight-binding theory in which the translational symmetry in three directions exists, the three-dimensional Fourier transformation is used to reduce the matrix size. In the present case, however, the translational symmetry along the z axis is lost, while the translational symmetry along the x and y directions remains. In such a case, it is convenient to introduce two-dimensional Fourier transformation as

$$a^{\dagger}_{l\boldsymbol{k}_{||}m} = \frac{1}{\sqrt{N}} \sum_i e^{i\boldsymbol{k}_{||}\cdot\boldsymbol{r}_i} a^{\dagger}_{im}, \quad (3)$$

$$a_{l\boldsymbol{k}_{||}m} = \frac{1}{\sqrt{N}} \sum_i e^{-i\boldsymbol{k}_{||}\cdot\boldsymbol{r}_i} a_{im}, \quad (4)$$

where $\boldsymbol{k}_{||}$ is a two-dimensional wave vector and $\boldsymbol{r}_i$ is the atomic position, and i runs through N atomic positions in a two-dimensional layer denoted by l. We set $\boldsymbol{k}_{||} = 0$ because the Stark ladders we are interested in are uniform states along the x and y directions. Using Eqs. (3) and (4), we can express the secular equation as

$$\det |H_{lm;l'm'} - E\delta_{ll'}\delta_{mm'}| = 0, \quad (5)$$

where diagonal elements of $H_{lm;l'm'}$ consist of the site energies and the second-neighbor transfer integrals of the atomic orbitals in the plane perpendicular to the z axis, and off-diagonal elements consist of the first-neighbor and the second-neighbor transfer integrals. We have to note here that the secular equation (5) has infinite size for an infinite number of superlattice periods. Since the number of periods for a real superlattice is finite, we consider a finite domain in the z direction. In the present study, we consider ten periods of $(GaAs)_n/(AlAs)_n$ superlattice. Solving the secular equation (5), we calculated the energy spectra and corresponding wave functions as linear combinations of atomic orbitals in various magnitudes of electric fields. In the present case, the spin-orbit interaction is neglected, and thus the Hamiltonian matrix can be decoupled into two irreducible parts,[17] where one consists of s and p_z orbitals and the other consists of p_x and p_y orbitals. Near the fundamental band edge, conduction minibands arise from the former and valence minibands arise from the latter.

III. CALCULATED RESULTS AND DISCUSSION

A. Γ-X mixing

Figure 1 shows a typical result of the calculated charge densities for the $(GaAs)_8/(AlAs)_8$ superlattice at 60 kV/cm, where square amplitudes of eigenvectors are plotted as a function of position. We note that the vertical axis is not to scale exactly but arbitrary in this figure. Doubly degenerated heavy hole valence states (denoted by Γ_{hh}), the first conduction states of the Γ edge of GaAs (Γ_c), and conduction states of the AlAs X point (X_c^1 and X_c^2) are shown in this figure, where we see that all these states are well localized in each GaAs and AlAs layer, respectively. The states Γ_c and X_c^2 mix with each other and are delocalized because they are close in terms of energy. According to the relative position between localized valence and conduction states, direct and indirect

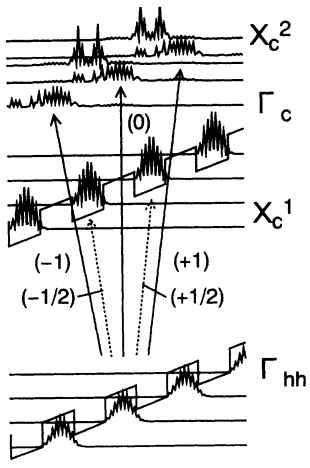

FIG. 1. Typical calculated charge densities of $(GaAs)_8/(AlAs)_8$ near the band edge at 60 kV/cm. Heavy hole valence states (Γ_{hh}), conduction states of the GaAs Γ edge (Γ_c), and first and second conduction states of the AlAs X edge (X_c^1 and X_c^2) are shown with oblique steps indicating the layers of GaAs and AlAs. The vertical axis is not exactly to scale.

transitions in real space which are denoted 0, $\pm 1/2$ and ± 1 would occur. These transitions will be discussed in the next section.

The X_c^i states (i=1, 2) have tails extending weakly in neighboring GaAs layers and the Γ_c states also have tails in neighboring AlAs layers. Partial charge of such a tail is an index of strength of the Γ-X mixing and we can easily evaluate this quantity from eigenvectors of Eq. (5). The partial charge of the X_c^i state is written as

$$C^i = \sum_l{}' \sum_m |c_{lm}^i|^2, \tag{6}$$

where c_{lm}^i is the eigenvector of the X_c^i state and summation of l is taken within atomic layers of GaAs. Although it is a rough treatment, the perturbation theory presents a good outlook of the Γ-X mixing. Let $|\Gamma_c^0\rangle$ ($|X_c^{i0}\rangle$) to be a state of Γ (X) band edge of an isolated GaAs (AlAs) layer in an electric field and E_Γ^0 (E_X^{i0}) to be the corresponding energy. When the GaAs layers and the AlAs layers are attached to form a superlattice, a perturbation $\mathcal{H}'$ occurs due to change of crystal potential, and thus $|\Gamma_c^0\rangle$ and $|X_c^{i0}\rangle$ mix with each other. Within the first order perturbation theory, we can express the states $|\Gamma_c\rangle$ and $|X_c^i\rangle$ of the superlattice as follows:

$$|\Gamma_c\rangle = |\Gamma_c^0\rangle + \sum_{i=1}^{2} \frac{\langle \Gamma_c^0|\mathcal{H}'|X_c^{i0}\rangle}{E_\Gamma^0 - E_X^{i0}} |X_c^{i0}\rangle, \tag{7}$$

$$|X_c^i\rangle = |X_c^{i0}\rangle + \frac{\langle X_c^{i0}|\mathcal{H}'|\Gamma_c^0\rangle}{E_X^{i0} - E_\Gamma^0} |\Gamma_c^0\rangle, \tag{8}$$

where we have neglected higher states.

From Eq. (8) the partial charge of the X_c^i state is expressed as

$$C^i = \frac{|\langle \Gamma_c^0|\mathcal{H}'|X_c^{i0}\rangle|^2}{(E_\Gamma - E_X^i)^2}, \tag{9}$$

where we have approximated as $E_\Gamma^0 - E_X^{i0} \approx E_\Gamma - E_X^i$. Equation (9) shows that the Γ-X mixing is dominated by two factors. One, which comes from the denominator of Eq. (9), is the so-called resonant effect, and depends on the electric field through $E_\Gamma - E_X^i$. The Γ-X mixing is strongly enhanced due to the resonant effect at an electric field where $E_\Gamma - E_X^i$ is small. Another factor comes from the numerator of Eq. (9), which depends on electric fields, superlattice structures, and miniband indices. However, behavior of $|\langle \Gamma_c^0|\mathcal{H}'|X_c^{i0}\rangle|^2$ cannot be intuitively understood. We have already seen in Fig. 1 the resonant mixing between Γ_c and X_c^1.

Figures 2(a) and 2(b) show the calculated partial charge of the X_c^i states of $(GaAs)_n/(AlAs)_n$ superlattices as functions of the electric fields. A large peak shown in each curve indicates the resonant coupling between the X_c^i state and the neighboring Γ_c state. Small deviations are due to other types of mixing such as mixing between X_c^1 and X_c^2. For the X_c^1 state, the Γ-X mixing occurs in a wide range of the electric fields as shown in Fig. 2(a). Shapes of the peaks for $(GaAs)_{10}/(AlAs)_{10}$ and $(GaAs)_{11}/(AlAs)_{11}$ are almost the same except for the peak position. The peak width of $(GaAs)_{10}/(AlAs)_{10}$ is slightly wider than that of $(GaAs)_{11}/(AlAs)_{11}$. These

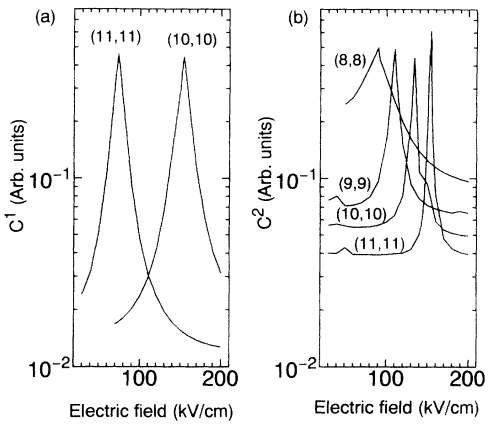

FIG. 2. (a) Partial charge of an X_c^1 state in GaAs layers calculated for a $(GaAs)_n/(AlAs)_n$ (n=10 and 11) superlattice. (b) Partial charge of an X_c^2 state in GaAs layers calculated for a $(GaAs)_n/(AlAs)_n$ (n=8–11) superlattice.

facts indicate that the Γ-X mixing exists even if $E_\Gamma - E_X^1$ is large, and that the strength of the Γ-X mixing decreases very slowly as n increases. The feature of the mixing between the X_c^2 state and the Γ_c state is quite different form that between the X_c^1 state and the Γ_c state as shown in Fig. 2(b). The peak for $(GaAs)_8/(AlAs)_8$ is quite broad, indicating a strong Γ-X mixing, and the peaks become sharper rapidly as n increases. From this result we can see that the strength of the Γ-X coupling between Γ_c-X_c^2 strongly depends on the superlattice structure; as n increases the strength of the Γ-X coupling is rapidly weakened. We also found that the character of the enhanced charge mainly reflects the s orbitals of As atoms. The partial charge of the X_c^2 state at off-resonant condition is larger than that of the X_c^1 state, reflecting the higher energy.

It is reported that the Γ-X mixing at zero electric field depends strongly on the parity of the states.[22,25] At zero electric field, parity of the X minibands alternates: X_c^1 is even (odd) and X_c^2 is odd (even), respectively, when n is an even (odd) number. On the other hand, Γ_c is an even state for any value of n. Reflecting the parity of the states, strength of the Γ-X mixing changes alternately with n. In the presence of electric fields, however, monotonous change with n instead of the alternation is seen because the symmetry is quite different due to the electric field.

B. Transition energies and transition probabilities

In addition to transition energies between localized states, we have evaluated matrix elements of optical transition by normal incident light with no particular polarization. Using calculated eigenvectors, the matrix elements are written as[26]

$$|M^2| = \frac{1}{2\pi} \int_0^{2\pi} |M^2(\theta)| d\theta, \tag{10}$$

with

$$M(\theta) = \sum_{lmm'} c_{lm}^{c*} c_{lm'}^{v} \left\langle \phi_m \left| \cos\theta \frac{\partial}{\partial x} + \sin\theta \frac{\partial}{\partial y} \right| \phi_{m'} \right\rangle , \tag{11}$$

where $c_{lm}^{c(v)}$ is an eigenvector of a conduction (valence) state. In calculating $|M|^2$ we set

$$\left\langle \phi_{px} \left| \frac{\partial}{\partial x} \right| \phi_s \right\rangle = \left\langle \phi_{py} \left| \frac{\partial}{\partial y} \right| \phi_s \right\rangle = 1, \tag{12}$$

and

$$\left\langle \phi_m \left| \frac{\partial}{\partial x} \right| \phi_{m'} \right\rangle = \left\langle \phi_m \left| \frac{\partial}{\partial y} \right| \phi_{m'} \right\rangle = 0, \tag{13}$$

for other combinations of atomic orbitals and partial derivative.

Calculated transition energies and transition probabilities for a $(GaAs)_8/(AlAs)_8$ superlattice are shown in Fig. 3, where transitions between Γ_{hh}-Γ_c, Γ_{hh}-X_c^1 and Γ_{hh}-X_c^2 are denoted by filled circles, open circles, and open squares, respectively. Although there are deviations from linear relations, the electric-field dependence of transition energies is well approximated as $meFd$ with an index $m = 0, \pm 1$ for the transition Γ_{hh}-Γ_c (d: superlattice period). Transitions Γ_{hh}-X_c^1 and Γ_{hh}-X_c^2 are also expressed as $meFd$ with $m = \pm 1/2$. Γ_{hh}-$\Gamma_c(0)$ and Γ_{hh}-$X_c^2(-1/2)$ show anticrossing at $F = 90 - 100$ kV/cm. Anticrossing between Γ_{hh}-$\Gamma_c(+1)$ and Γ_{hh}-$X_c^2(+1/2)$ and kinking in Γ_{hh}-$\Gamma_c(-1)$ take place at the same electric field. These are due to strong mixing between the Γ_c and X_c^2 states, which are already shown in Figs. 1 and 2(b). In addition to the strong Γ-X mixing, the Γ_c and X_c^2 states are close in terms of energy in a wide region of electric fields. Thus the Γ-X mixing between them has a large effect on the transition energies of Γ_{hh}-Γ_c and Γ_{hh}-X_c^2. Such strong mixing between transitions Γ_{hh}-Γ_c and Γ_{hh}-X_c^2 has been observed.[27]

Behavior of the transition probability is quite complicated. As a gross feature, the direct transition in real space Γ_{hh}-$\Gamma_c(0)$ becomes stronger, and other oblique transitions become weak with increasing electric fields. Such behavior is due to the fact that the wave functions are strongly confined in the layers at larger electric fields. However, the interband mixing largely modulates the transition probabilities. $|M|^2$ of Γ_{hh}-$X_c^2(-1/2)$ is strongly enhanced in a wide region of electric fields due to the Γ-X mixing. $|M|^2$ of Γ_{hh}-$\Gamma_c(+1)$ and that of Γ_{hh}-$X_c^2(+1/2)$ drastically change at F=90–100 kV/cm where the anticross takes place. Due to the mixing effect, there is a large difference in a transition probability between the plus index state and the minus index state. Γ_{hh}-$\Gamma_c(+1)$ has a larger transition probability than Γ_{hh}-$\Gamma_c(-1)$ below 90 kV/cm, and the relation is reversed above 100 kV/cm. Γ_{hh}-$X_c^2(-1/2)$ has a much larger transition probability than Γ_{hh}-$X_c^2(+1/2)$. The transitions Γ_{hh}-$X_c^1(\pm 1/2)$ have much smaller probabilities compared with other transitions because the resonant mixing between Γ_c and X_c^1 does not occur in electric fields lower than 200 kV/cm. This fact is consistent with the report of Shields *et al.* in which the transitions Γ_{hh}-X_c^1 are observed as very weak signals.

Transition energies and transition probabilities of $(GaAs)_{10}/(AlAs)_{10}$ are shown in Fig. 4. Compared to $(GaAs)_8/(AlAs)_8$, the transition energy for Γ_{hh}-Γ_c is lower. This feature leads to the situation where Γ_{hh}-$\Gamma_c(0)$, Γ_{hh}-$X_c^1(+1/2)$ and Γ_{hh}-$X_c^2(-1/2)$ cross with each other at almost the same strength of the electric fields 130–150 kV/cm. Both the transition probability of Γ_{hh}-$X_c^1(+1/2)$ and that of Γ_{hh}-$X_c^2(-1/2)$ are strongly enhanced at these electric fields, while Γ_{hh}-$X_c^1(-1/2)$ and Γ_{hh}-$X_c^2(+1/2)$ are weak, although they

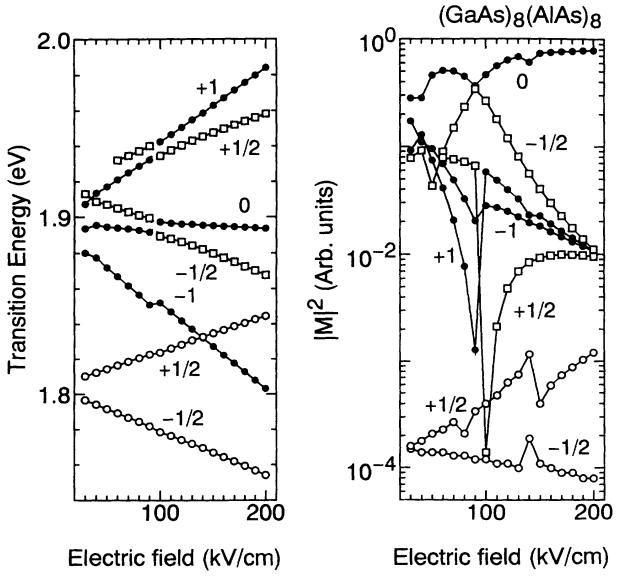

FIG. 3. Transition energies (left-hand side) and optical matrix elements (right-hand side) calculated for a $(GaAs)_8/(AlAs)_8$ superlattice. Filled circles, open circles, and open squares denote transitions Γ_{hh}-Γ_c, Γ_{hh}-X_c^1, and Γ_{hh}-X_c^2, respectively. Indices 0, ±1, and ±1/2 denote relative position between localized states.

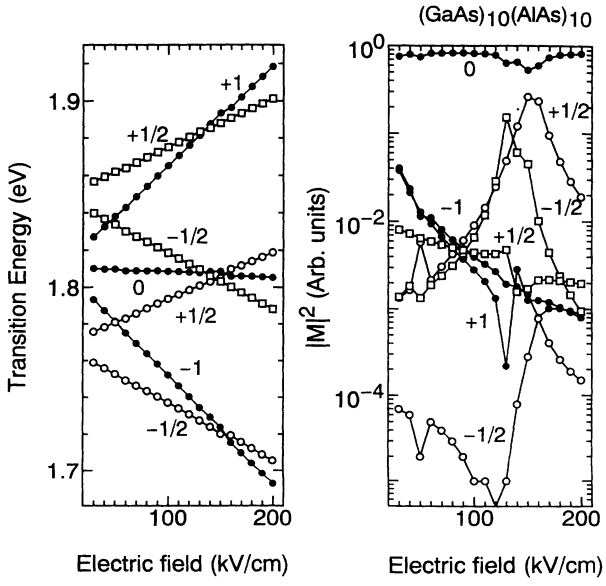

FIG. 4. Transition energies (left-hand side) and optical matrix elements (right-hand side) calculated for a $(GaAs)_{10}/(AlAs)_{10}$ superlattice.

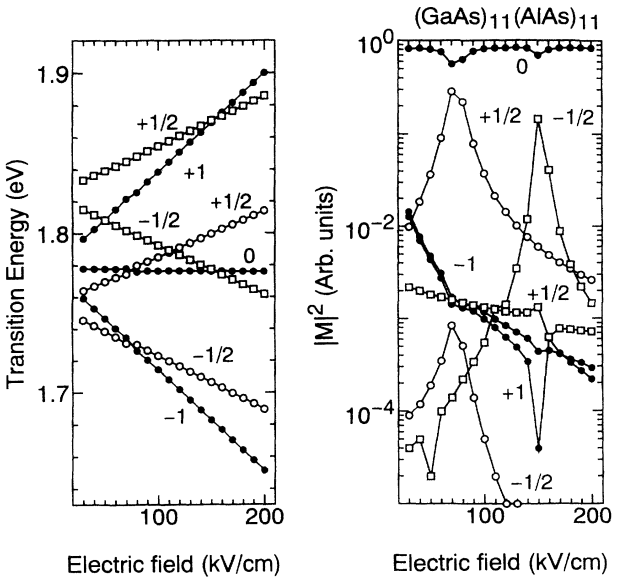

FIG. 5. Transition energies (left-hand side) and optical matrix elements (right-hand side) calculated for a $(GaAs)_{11}/(AlAs)_{11}$ superlattice.

cross Γ_{hh}-$\Gamma_c(+1)$and Γ_{hh}-$\Gamma_c(-1)$, respectively. Thus the asymmetry in transition probabilities (the difference in the transition probabilities) between Γ_{hh}-$X_c^2(-1/2)$ and Γ_{hh}-$X_c^2(1/2)$ and that between Γ_{hh}-$X_c^1(-1/2)$ and Γ_{hh}-$X_c^1(1/2)$ is also seen in this case. On the other hand, asymmetric behavior between Γ_{hh}-$\Gamma_c(+1)$ and Γ_{hh}-$\Gamma_c(-1)$ is small.

Transition energies and transition probabilities of $(GaAs)_{11}/(AlAs)_{11}$ are shown in Fig. 5. Due to the Γ-X mixing, Γ_{hh}-$X_c^1(+1/2)$ is enhanced in a wide range of electric fields, while Γ_{hh}-$X_c^2(-1/2)$ is enhanced sharply around $F \sim 150$ kV/cm. This is consistent with the result shown in Sec. III A; as n increases the resonant mixing between Γ_c-X_c^2 becomes weak more rapidly than that between Γ_c-X_c^1. In addition, $|M|^2$ of Γ_{hh}-$\Gamma_c(\pm1)$is smaller than that of $(GaAs)_8/(AlAs)_8$ and $(GaAs)_{10}/(AlAs)_{10}$. Asymmetry between Γ_{hh}-$\Gamma_c(+1)$ and Γ_{hh}- $\Gamma_c(-1)$ is smaller than that of $(GaAs)_8/(AlAs)_8$ and $(GaAs)_{10}/(AlAs)_{10}$. These are due to the thicker AlAs barriers, which reduce the penetration of the localized state.

In summary, we evaluated the strength of the electric-field-induced Γ-X mixing between Stark ladder states using the second-neighbor tight-binding method. We found that the Γ-X mixing remarkably depends on superlattice structures and indices of the X minibands. Optical transition energies and transition probabilities between Stark ladders are strongly affected by the Γ-X mixing: anticross in transition energies and asymmetry in transition probabilities are expected. Results shown in the paper may depend on the tight-binding parameters we chose. Lu and Sham noted that their parameters lead to stronger Γ-X mixing than other parameters do. Furthermore, the effect of charge redistribution may be important. It is a difficult to consider the effect of charge redistribution in a self-consistent manner. By comparing calculated results with experimental data precisely, the importance of these points will be clear.

ACKNOWLEDGEMENT

One of the authors (M.M.) acknowledges the financial support of the Murata Science Foundation.

[1] G. H. Wannier, Phys. Rev. **117**, 432 (1960).
[2] J. Zak, Phys. Rev. Lett. **20**, 1477 (1968); Phys. Rev. **181**, 1366 (1969).
[3] M. Saitoh, J. Phys. C **5**, 914 (1972).
[4] H. Fukuyama, R. A. Bari, and H. C. Fogedby, Phys. Rev. **8**, 5579 (1973).
[5] T. Kawaguchi and M. Saitoh, J. Phys. C **3**, 9371 (1991).
[6] S. Maekawa, Phys. Rev. Lett. **24**, 1175 (1970).
[7] F. Agullo-Rueda, E. E. Mendez, and J. M. Hong, Phys. Rev. B **40**, 1357 (1989).
[8] E. E. Mendez, F. Agullo-Rueda, and J. M. Hong, Appl. Phys. Lett. **56**, 2545 (1990).
[9] J. Bleuse, P. Voisin, M. Allovon, and M. Quillec, Appl. Phys. Lett. **53**, 2632 (1988).
[10] P. Voisin, J. Bleuse, C. Bouche, S. Gaillard, C. Albert, and A. Regreny, Phys. Rev. Lett. **61**, 1639 (1988).
[11] J. Bleuse, G. Bastard, and P. Voisin, Phys. Rev. Lett. **60**, 220 (1988).
[12] A. J. Shields, P. C. Klipstein, M. S. Skolnick, G. W. Smith, and C. R. Whitehouse, Phys. Rev. B **42**, 5879 (1990).
[13] D. M. Whittakker, M. S. Skolnick, G. W. Smith, and C. R. Whitehouse, Phys. Rev. B **42**, 3591 (1990).
[14] I. Tanaka, M. Nakayama, H. Nishimura, K. Kawashima, and K. Fujiwara, Phys. Rev. B **46**, 7656 (1992).
[15] A. M. Fox, D. A. B. Miller, G. Livescu, J. E. Cunningham, and W. Y. Jan, Phys. Rev. B **44**, 6231 (1991).
[16] D. C. Hutchings, Appl. Phys. Lett. **55**, 1082 (1989).
[17] M. Morifuji, Y. Nishikawa, C. Hamaguchi, and T. Fujii, Semicond. Sci. Technol. **7**, 1047 (1992).
[18] K. Hirabayashi, J. Phys. Soc. Jpn. **27**, 1475 (1969).
[19] P. Vogl, P. Hjalmarson, and J. D. Dow, J. Phys. Chem. Solids **44**, 365 (1983).
[20] K. E. Newmann and J. D. Dow, Phys. Rev. B **36**, 1929 (1984).
[21] Jian-Bai Xia and Yia-Chung Chang, Phys. Rev. B **42**, 1781 (1990).
[23] M. Yamaguchi, M. Morifuji, H. Kubo, K. Taniguchi, C. Hamaguchi, C. Gmachl, and E. Gornik, Solid State Electron. **37**, 839 (1994).
[24] P. O. Lödin, J. Chem. Phys. **18**, 365 (1950).
[25] T. Matsuoka, T. Nakazawa, T. Ohya, K. Taniguchi, C. Hamaguchi, H. Kato, and Y. Watanabe, Phys. Rev. B **43**, 11 798 (1991).
[26] H. Fujimoto, C. Hamaguchi, T. Nakazawa, K. Taniguchi, K. Imanishi, H. Kato, and Y. Watanabe, Phys. Rev. B **41**, 7593 (1991).
[27] M. Yamaguchi, H. Nagasawa, M. Morifuji, K. Taniguchi, C. Hamaguchi, C. Gmachl, and E. Gornik, Semicond. Sci. Technol. (to be published).